Estimation of the surface strain distribution in upsetting

Estimation of the Surface Strain Distribution in Upsetting

J. A. G. Kals, T. H. Eindhoven/NL (1)

Summary: The cold upsetability is limited by crack initiation in the free surface. Even equally typified materials can behave in a significantly different manner. Usually the upsetting test is applied but a number of questions is still open. In normal testing the deformation is qualified arbitrarily for the test piece as a whole by measuring the (critical) reduction in height. Cracks, however, arise from a local situation and thus must be studied in relation with local values of physical quantities. The relation between the reduction in height and the local strains has to be taken into account by the design of a sound testing procedure which satisfies practical needs. An attempt is made to predict the actual strains on the base of a geometrical consideration of the surface growth. Although this will not provide a final solution a few questions are clarified. Particularly the effect of the initial geometry on the strainpath appears to be important and has to be taken into account by continued investigations of surface instability and crack phenomena.

INTRODUCTION.

If the upsetting test is used to establish the stress-strain relation of metals the utility of the provided data is mostly acceptable. The stress-strain curve represents average values over the test piece if the test is carried out in a proper way. The situation is different, however, if the crack initiation in upsetting is studied in order to establish the formability of metals. In this case one has to take into account that the initiation of a crack is due to the local stress and strain situation and with certainty not to some overall values of the load and deformation. Only the last ones, however, can be measured easily.

Unfortunately the relation between the overall deformation and the local strain values is effected by many factors such as strain hardening, friction conditions in the contact planes, process instability, surface instability etc. in a very complicated manner. One of these factors was investigated by Baqué [1]. After careful observation of the growth of micro pores in the free surface of the test piece by means of an electron microscope, he supposed a relation between instable strain concentration ("necking") and the initiation of cracks. Since Gillemot [2] a.o. suggested a relation between crack initiation and a critical level of dissipated specific energy this seems to be a resonable representation. Nevertheless, the strain path of the cracking material has to be established experimentally in order to confirm things a posteriori. Therefore the approach by Baqué cannot be used to predict crack initiation.

Observations of the deformation behaviour of the free surface in upsetting tests on metals and model materials made clear that the surface layers of a test piece deform in a different way compared with the material within the test piece. An attempt is made in the following to explain the tendency of the strainpath of the free surface elements by considering the surface area of the test piece only.

THE CHANGE OF THE SURFACE AREA.

For a rigid plastic material and a circular test piece the volume can be expressed in the original or current dimensions during upsetting:

(1) $$V = \frac{\pi}{4} H_o D_o^2 = \frac{\pi}{4} H D^2 = \text{constant},$$

where H_o, H = initial and current height.
D_o, D = initial and current diameter.

Further:

(2) $$D = 2\sqrt{\frac{V}{\pi H}}$$

The total surface area A of the test piece is

(3) $$A = A_c + A_f = \frac{\pi}{2} D(D + 2H)$$

where A_c = tool contact area (at both ends).
A_f = free cylindrical surface area.

Combining (2) and (3) we find

(4) $$\boxed{A = 2\pi \sqrt{\frac{V}{\pi H}} \left(\sqrt{\frac{V}{\pi H}} + H\right)}$$

As can be shown easily this expression provides a minimum value for A under the condition

(5) $$D_m = H_m = \sqrt[3]{\frac{4V}{\pi}}$$

which represents a test piece profile nearest to a sphere. So we can conclude that the total surface area A decreases initially if $H_o > D_o$ and increases after H = D is reached. This effect is illustrated in Fig. 1.

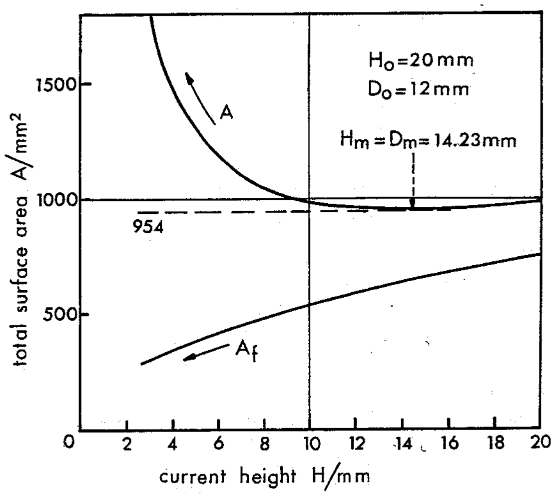

Fig. 1. Graphical representation of eq. (4) for an arbitrary set of numbers.

THE DEVELOPMENT OF THE FREE SURFACE.

Cracks are mostly initiated in the free part A_f of the test piece which is not in contact with the tool plates. The falling off of the area A_f in the cause of the upsetting process is also represented in Fig. 1. This seems to contradict the appearance of local instability. Necking, namely, generally demands an increase in area because actually it is an instable concentration of surface growth. By means of the grid technique, however, one can observe in the edge region of the test piece that the free surface continuously moves over into the contact plane under the condition of friction. This happens to an extreme extent for sticking conditions in the contact plane. Many times sticking is realised artficially, for example by roughening the tool plates with a pattern of concentric grooves, a.o. for reasons of test repeatability. Therefore this test procedure is especially investigated in the following. See Fig. 2. and lit. [5].

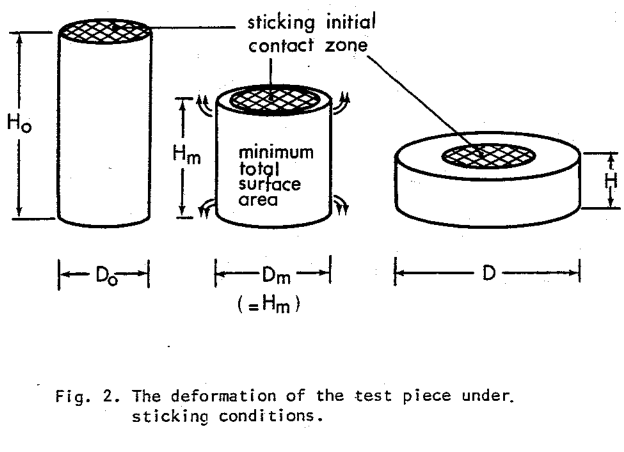

Fig. 2. The deformation of the test piece under sticking conditions.

Considering that all surface elements in the contact area are constant in this case, we have to take into account that the progressive growth of the contact area has to be raised entirely in the (decreasing) free surface and possibly also partly in the edge area.

If some particular edge mechanism is neglected for the time being we have to conclude that the average surface strain in the free surface must be positive and progressively increasing for $D > H$ and $dD > 0$ in spite of the decrease of the free surface area. For any small element S_f of the free surface A_f we can write:

$$(6) \quad \frac{dS_f}{S_f} = d\varepsilon_\theta + d\varepsilon_a = - d\varepsilon_r,$$

where θ, a and r indicate respectively the circumferencial, the axial and the radial direction. For $\sigma_r = 0$ we have further

$$(7) \quad d\varepsilon_r = - \frac{d\lambda}{2} (\sigma_\theta + \sigma_a), \text{ and}$$

$$(8) \quad \frac{dS_f}{S_f} = \frac{d\lambda}{2} (\sigma_\theta + \sigma_a)$$

So if additional surface is raised somewhere in the outer surface the following condition for the local principal surface stresses holds:

$$(9) \quad \sigma_\theta + \sigma_a > 0$$

This underlines that allowance has to be made for a free surface behaviour which differs quite considerably from the deformation of the test piece as a whole.

THE AVERAGE STRETCHING OF THE FREE SURFACE.

From measurements it could be established that the free surface extends rather homogeneously. If, for the sake of simplicity, a uniform deformation in the outer surface is assumed in addition to perfect sticking in the contact zone, we have:

$$(10) \quad \frac{dA}{A_f} = \frac{dA_c + dA_f}{A_f} = \frac{dS_f}{S_f}$$

where from eq. (4)

$$(11) \quad dA = 2\pi \sqrt{\frac{V}{\pi H}} \left(\frac{1}{2} - \frac{1}{H} \sqrt{\frac{V}{\pi H}}\right) dH,$$

and from eqs. (2) and (3)

$$(12) \quad A_f = \pi D H = 2\pi H \sqrt{\frac{V}{\pi H}}$$

Substitution of eqs. (11) and (12) in (10) leads with (6) to

$$(13) \quad d\varepsilon_r = - \frac{dS_f}{S_f} = \left(\frac{1}{H^2} \sqrt{\frac{V}{\pi H}} - \frac{1}{2H}\right) dH$$

Integration and the substitution of eq. (1) finally provides the expression for the radial strain:

$$(14) \quad \varepsilon_r = -\frac{1}{3} \frac{D_o}{H_o} \left[\left(\frac{H_e}{H_o}\right)^{-3/2} - 1\right] - \ln \sqrt{\frac{H_e}{H_o}}$$

Introducing φ for the logarithmic overall degree of deformation the following expression is obtained.

$$(15) \quad \boxed{\varepsilon_r = - \frac{1}{3} \frac{D_o}{H_o} \left[\exp.\left(- \frac{3}{2}\varphi\right) - 1\right] - \frac{\varphi}{2}}$$

The tendency of this relation is represented in Fig. 3.

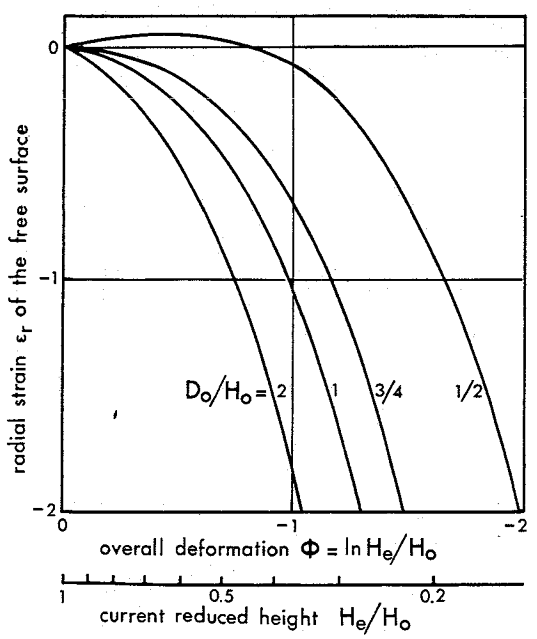

Fig. 3. Representation of eq. (15).

From this graph it becomes clear that - under the conditions mentioned before - the free surface is stretched considerably (see eq. (6)). A further important conclusion suggested by Fig. 3 is that the initial shape of the test cylinder strongly influences the strain path of the free surface elements. So, test results do not only depend on the degree of overall deformation etc. but also on the initial shape of the test piece. This seems to imply similarity problems in using formability data in the development of production processes.

THE AVERAGE AXIAL AND HOOP STRAIN OF THE FREE SURFACE.

In order to enable a first check of the developed model in using the grid technique the expressions for the surface strains ε_θ and ε_a are now necessary. From eq. (14) follows with (6)

$$(16) \quad \varepsilon_\theta + \varepsilon_a = \frac{1}{3} \frac{D_o}{H_o} \left[\left(\frac{H_e}{H_o}\right)^{-3/2} - 1\right] + \ln \sqrt{\frac{H_e}{H_o}}$$

with eq. (1) we obtain

$$(17) \quad D_e = D_o \sqrt{\frac{H_o}{H_e}}, \text{ so}$$

$$(18) \quad \boxed{\varepsilon_\theta = \ln \frac{D_e}{D_o} = \ln \sqrt{\frac{H_o}{H_e}}}$$

Substitution of (18) in (16) yields the expression for the axial surface strain:

$$(19) \quad \boxed{\varepsilon_a = \frac{1}{3} \frac{D_o}{H_o} \left[\left(\frac{H_e}{H_o}\right)^{-3/2} - 1\right] + \ln \frac{H_e}{H_o}}$$

The strain path according to eqs. (18) and (19) is represented in Fig. 4 for different values of the initial height/diameter ratio of the test piece. Considering this graph, however, one has to take into account that the deformation behaviour represented is an extreme case. The validity restrictions as already mentioned before are:

1. sticking conditions in the contact area
2. uniform deformation of the free surface
3. continuously cylindrical shape of the test piece
4. absence of any separate surface growth in the edge region.

Because of the obviously curved strain-paths the straight lines for ε_r = constant cannot be used as local instability boundaries [3]. Nevertheless these underline the probability of necking by an exhaust of strain hardening capacity of the material.

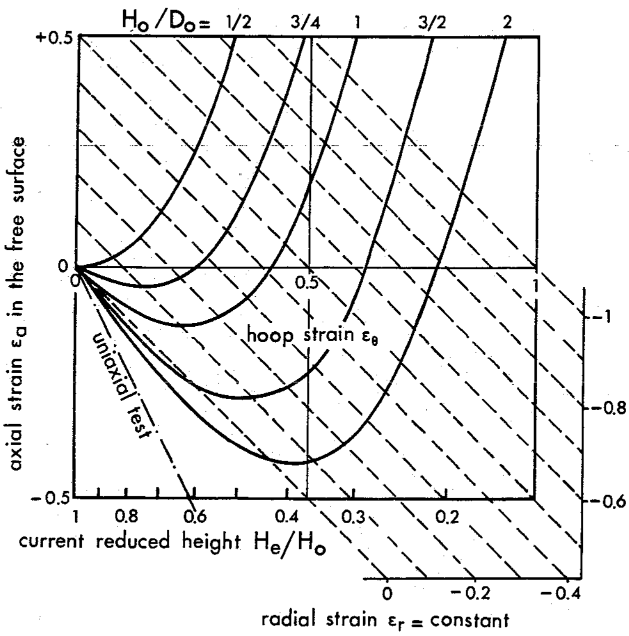

Fig. 4. Strain path representation acc. to eqs. (15), (18) and (19). Minima for H/D = 1/2 ($d\varepsilon_a = 0$).

Although large positive axial strains according to Fig. 4 could be observed for some pastlike model materials, the behaviour of metals (copper and steel) appeared to be overdone by the curves as calculated above. From the validity restrictions mentioned above particularly the deformation in the edge region is unknown and should be taken into account.

AN EDGE ZONE ADAPTATION.

In behalf of this surveying study it's desirable to have a simple model representing the possible local increase of surface elements passing by the edge region. Such a model is suggested by the crack planes as observed in brass which has a low ductility.

For H ≥ D the angle between the contact plane and the cone shaped crack plane through the edge is 45°. For H < D this angle decreases to an amount ≥ arctan (H/D). The surface elements of the free surface are considered to be projected on the contact-plane in such a way that the direction of projection is given by the shear angle in the edge of the test piece. For H < D this implies an increase in area of the passing surface elements. If the enlargement factor is called ψ, we have

(20a) $\psi = 1$ for $H \geq D$

(20b) $\psi = D/H$ for $H \leq D$ in the first instance

The discontinuity in the surface growth can now be worked up in the model. The total surface increase of the test piece has but partly to be raised in the free surface. Eq. (10) turns into

$$(21)\quad \frac{dA}{A_f} = \psi \frac{dS_f}{S_f}$$

with eqs. (6), (11) and (12) we have:

$$(22)\quad d\varepsilon_r = \frac{1}{\psi}\left(\frac{1}{H^2}\sqrt{\frac{V}{\pi H}} - \frac{1}{2H}\right) dH$$

with

$$(23)\quad d\varepsilon_\theta = -\frac{dH}{2H}$$

follows next

$$(24)\quad d\varepsilon_a = -(d\varepsilon_r + d\varepsilon_\theta) = \left[\left(1 + \frac{1}{\psi}\right)\frac{1}{2H} - \frac{1}{\psi H^2}\sqrt{\frac{V}{\pi H}}\right] dH$$

By substitution of eq. (20b) proceeds from this

$$(25)\quad d\varepsilon_a = \frac{1}{4}\left(\frac{V}{\pi H}\right)^{-1/2} dH$$

Integration from the intermediate height H_m down to any current value H_e gives

$$(26)\quad \Delta\varepsilon_a = \frac{1}{3}\frac{H_m}{D_m}\left[\left(\frac{H_e}{H_m}\right)^{3/2} - 1\right]$$

with eq. (5) this turns into

$$(27)\quad \Delta\varepsilon_a \Big/_{H_m}^{H_e} = \frac{1}{3}\left(\frac{H_e}{D_e} - 1\right)$$

So, for a test piece with $H_o/D_o > 1$ the strain path between H_m and the smaller current value H_e can be calculated according to:

$$\varepsilon_a = \varepsilon_a \Big/_{H_o}^{H_m} + \Delta\varepsilon_a \Big/_{H_m}^{H_e}$$

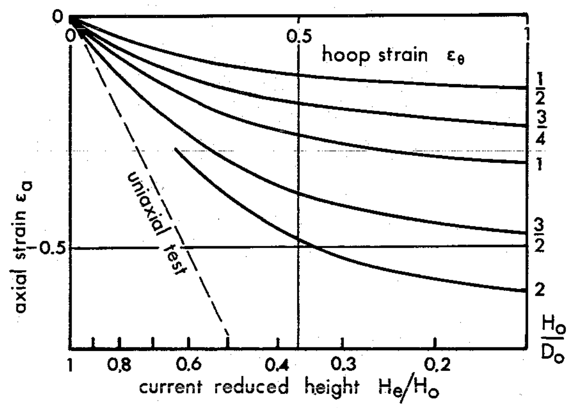

Fig. 5. Calculated strain paths acc. to eqs. (28) and (30) for different H_o/D_o ratios.

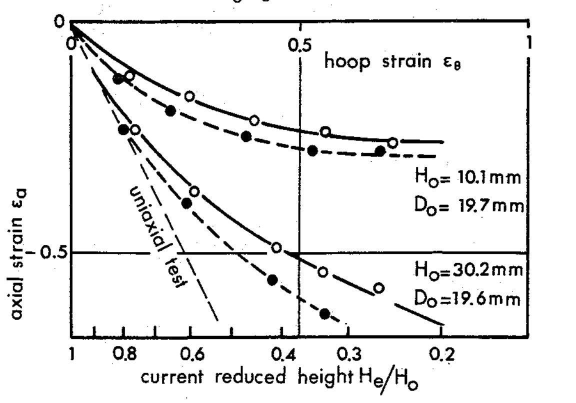

Fig. 6. Measured strain path for two copper test pieces. Initial grid elements 1 mm square. Local values are represented by open circles and average values over the momentary free surface by closed circles. The local values are measured in the middle.

By substitution of (19) for $H_e = H_m$ and (27) this can be worked up to

$$(28)\quad \varepsilon_a = \frac{1}{3}\left[\frac{H_o}{D_o}\left(\frac{H_e}{H_o}\right)^{3/2} - \left(\frac{H_o}{D_o}\right)^{-1} - 2\ln\frac{H_o}{D_o}\right] \qquad \text{for } H_o > D_o$$

So, with eq. (18) for ε_θ this provides the strain path between H_m and H_e. The part of the strain path between H_o and H_m can be fixed with eq. (19) in the same way as carried out for Fig. 4. The point where (19) passes to (28) is easily found from eqs. (1) and (5) to

$$(29)\quad \frac{H_m}{H_o} = \left(\frac{H_o}{D_o}\right)^{-2/3}$$

In the other less complicated case that $H_o/D_o \leq 1$ eq. (25) can be integrated directly from H_o to H_e. The following equation is obtained:

$$(30)\quad \varepsilon_a = \frac{1}{3}\frac{H_o}{D_o}\left[\left(\frac{H_e}{H_o}\right)^{3/2} - 1\right] \qquad \text{for } H_o \leq D_o$$

Some curves according to the adjusted strain path equations (28) and (30) are represented in Fig. 5.

Because of the time consuming character of the grid measurements only a limited number of experiments has been carried out. Within the scope of this orientation this will do. Both the local and the average strain values have been established. The results are represented in Fig. 6. Similar results have been obtained by Kivivuori et al. [4].

CONCLUSIONS.

- Taking into account that almost exclusively the surface deformation has been considered, the tendencies of the strain paths in the free surface could be explained remarkably well. Maybe this can be understood as an indication that a metal surface leads its own life to some extent.
- The quantitative correspondence of the calculated and measured strain paths is not perfect. It can be improved numerically by using a generalised linear function instead of eq. (20b). A limited rotation of the direction of projection of the edge elements, as a result of preceding strain hardening in the earlier shear planes or the neglected convexity of the free surface, is plausible. Further problems, such as the influence of the groove pattern in the contact area and a sometimes remarkable excentricity also handicap the accuracy of the results. It can be expected further that the strain hardening capacity of the material influences the extent of strain concentration in de edge zone. These effects will be subjected to further investigations.
- In the first instance the model developed offers possibilities for the analysis of redundant work and in doing so for necking and crack initiation also.
- In choosing optimal conditions for an upsetting process, either for production purposes or for a testing procedure, the initial height/diameter ratio should be considered as an important factor.

ACKNOWLEDGEMENT.

The author is grateful to Mr. M. Smeets for his help and the realization of the experiments.

REFERENCES.

[1]. P. Baqué, B. Roncin: Instabilités d'Ecoulement sur une Surface Libre et Critère de Fracture. Annals of the CIRP, 24/1, 213 (1975).
[2]. L.F. Gillemot: Criterion of Crack Initiation and Spreading. Engineering Fracture Mechanics, 8, 239 (1976).
[3]. J.A.G. Kals, P.C. Veentra: On the Critical Radius in Sheet Bending. Annals of the CIRP, 23/1, 55 (1974).
[4]. S. Kiviuori, M Sulonen: Formability Limits and Fracturing Modes of Uniaxial Compression Specimens. Annals of the CIRP, 27/1, 141 (1978).
[5]. E. Dannenmann, M. Blaich: Verfahren zur Prüfung der Kaltstauchbarkeit. Draht, 29, 703 (1978).